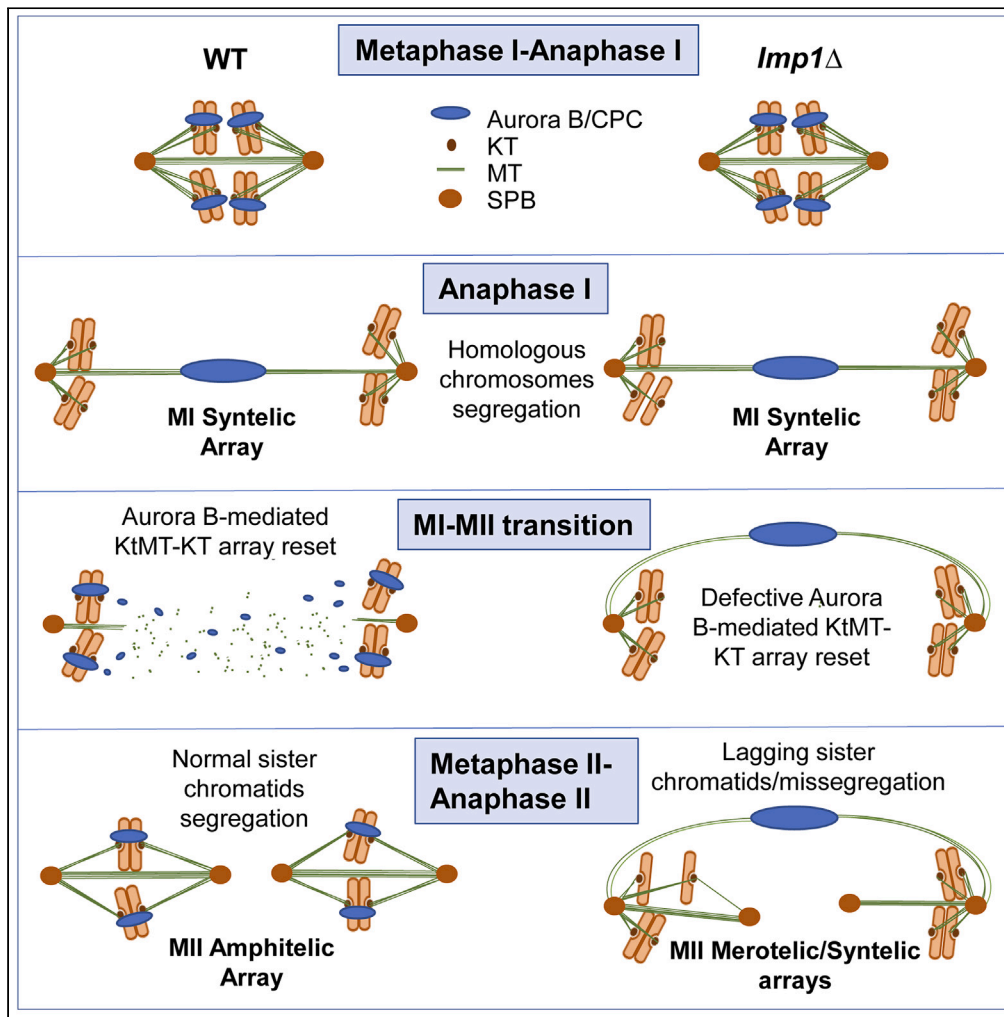**Article**

Aurora B kinase erases monopolar microtubule-kinetochore arrays at the meiosis I-II transition

Sergio Villa-Consuegra, Víctor A. Tallada, Juan Jimenez

valvtal@upo.es (V.A.T.)
jjimmar@upo.es (J.J.)

Highlights

Aurora B kinase re-localizes from mid-spindle to kinetochores at anaphase I exit

Aurora B spindle midzone releases requires importin α Imp1 function

Kinetochore re-located Aurora B erases monopolar arrays at meiosis interkinesis

Delaying Aurora B re-location leads to chromosome segregation errors in meiosis II

Article

Aurora B kinase erases monopolar microtubule-kinetochore arrays at the meiosis I-II transition

Sergio Villa-Consuegra,[1] Víctor A. Tallada,[1,*] and Juan Jimenez[1,2,*]

SUMMARY

During meiosis, faithful chromosome segregation requires monopolar spindle microtubule-kinetochore arrays in MI to segregate homologous chromosomes, but bipolar in MII to segregate sister chromatids. Using fission yeasts, we found that the universal Aurora B kinase localizes to kinetochores in metaphase I and in the mid-spindle during anaphase I, as in mitosis; but in the absence of an intervening S phase, the importin α Imp1 propitiates its release from the spindle midzone to re-localize at kinetochores during meiotic interkinesis. We show that "error-correction" activity of kinetochore re-localized Aurora B becomes essential to erase monopolar arrangements from anaphase I, a prerequisite to satisfy the spindle assembly checkpoint (SAC) and to generate proper bipolar arrays at the onset of MII. This microtubule-kinetochore resetting activity of Aurora B at the MI-MII transition is required to prevent chromosome missegregation in meiosis II, a type of error often associated with birth defects and infertility in humans.

INTRODUCTION

In eukaryotic cells, the microtubule-based mitotic spindle generates forces to align the condensed chromosomes at the metaphase plate and then pull the sister chromatids in opposite directions to segregate them into two daughter cells during anaphase. The spindle is composed of two types of microtubules. Dynamic kinetochore microtubules (KtMTs) capture and pull chromosomes, whereas interpolar microtubules (ipMTs) connect and separate the two spindle poles.[1–3] The kinetochore is the key structure assembled at the centromere that mediates the interactions of chromosomes with the KtMTs of the spindle. This large proteinaceous structure is composed of two submodules: the inner and outer kinetochore. While the inner kinetochore persists with centromeres throughout the cell cycle, the outer kinetochore attaches microtubules to the inner kinetochore and assembles only to condensed chromosomes during mitosis.[4] In fission yeast, however, in contrast to those of metazoans, most of the kinetochore components tend to be constitutive throughout the mitotic cell cycle, and only few outer factors associate at mitosis.[5–7]

Kinetochores can initially bind to microtubules in any configuration, but in mitosis, precise chromosome segregation requires that the outer kinetochores of sister chromatids ultimately bind to KtMTs from opposite spindle poles (amphitelic arrangement). These bipolar junctions are carefully regulated by the error-correction mechanism driven by Aurora B kinase (Ark1)[8,9] and the spindle assembly checkpoint (SAC).[10,11] Incorrect arrangements are destabilized and only correct bioriented arrays are stabilized, ensuring accurate chromatids segregation.[12] The spindle segregates the sister chromatids during anaphase, and once segregated, the chromosomes decondense, and the KtMT-kinetochore complexes disassemble to initiate a new cell cycle. In *S. pombe*, centromeres are clustered at the spindle pole bodies (SPBs) in the interphase of mitotic cycles.[13]

Meiosis is a conserved event of sexual reproduction in eukaryotic organisms. Unlike the mitotic cycle, in which M-phase and S-phase alternate, meiosis consists of two rounds of chromosome segregation after a single round of DNA replication, leading to the generation of haploid gametes from diploid germ cells. In meiosis I (MI), homologous chromosomes segregate toward opposite poles (reductional segregation), whereas in meiosis II (MII), sister chromatids separate from each other (equational segregation).[14] These different types of chromosome segregation depend on different arrays of spindle attachment to chromosomes. While the bipolar MI segregation of homologous chromosomes requires sister kinetochores of each chromosome to be mono-oriented to capture microtubules from the same pole (syntelic arrangement),[15] in MII, biorientation occurs similarly to mitosis in that sister kinetochores are attached to microtubules from opposite spindle poles (amphitelic arrangement).[16] These distinct MI and MII arrangements of KtMTs-kinetochores are critical to produce haploid cells by two consecutive meiotic divisions. However, the events and mechanisms regulating the dynamics of these different KtMT-Kinetochore arrays at the time interval from the exit of anaphase I to the onset of premetaphase II (the MI-MII transition) are not well understood. In this study, by using *imp1Δ* mutants that keep Ark1 sequestered at the midzone of hyperstable MI spindles,[17] we demonstrate that the relocation of
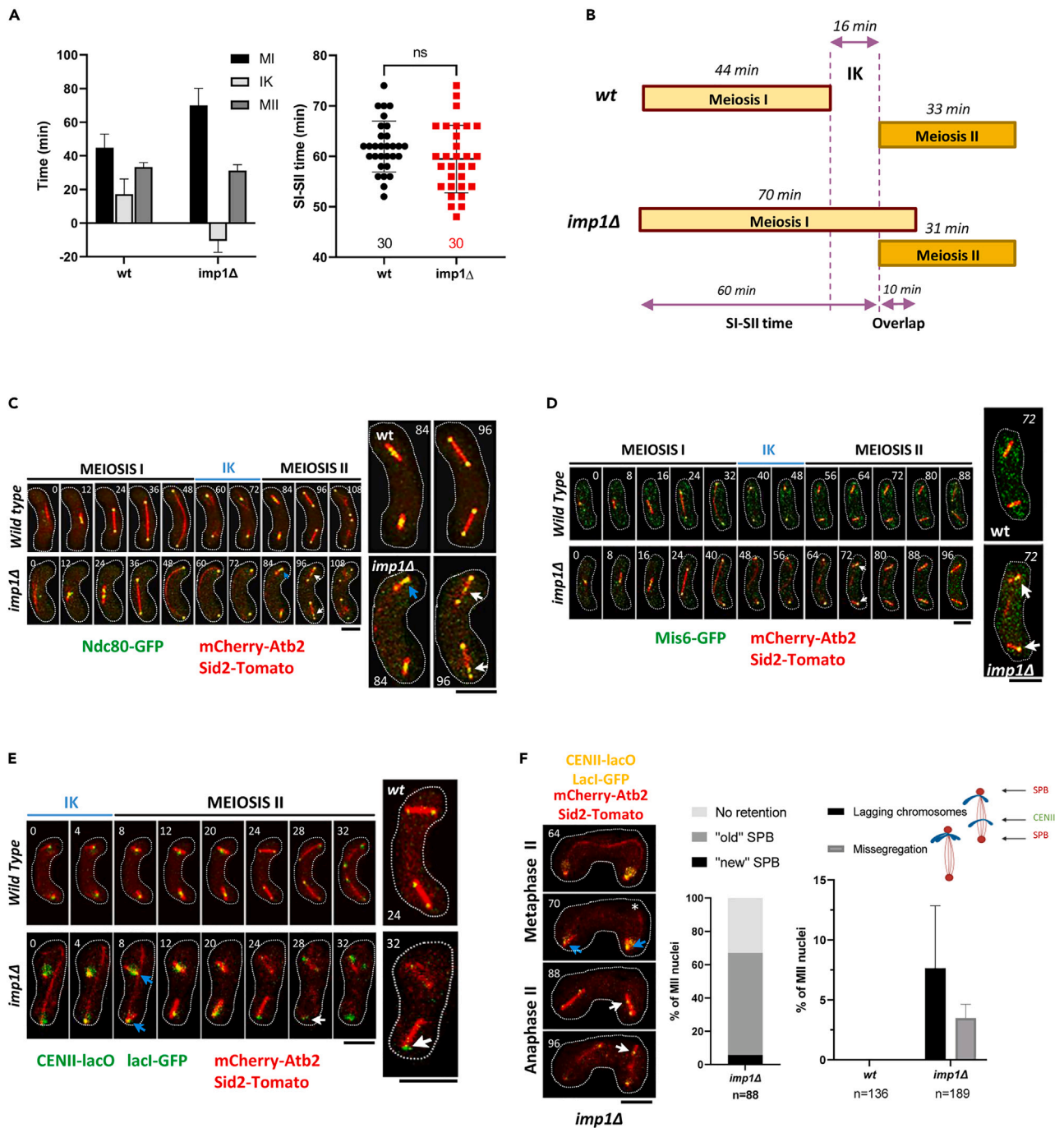
Figure 1. Effects of delayed MI spindle disassembly on sister chromatid segregation

(A) Duration (minutes) of meiosis I (MI), interkinesis (IK) and meiosis II (MII) in h90 wild-type (wt; n = 30) versus h90 imp1Δ (n = 30) zygotic cells measured from the spindle (mCherry-atb2) and SPB (Sid2-Tomato) dynamics. imp1Δ zygotic cells show a negative IK time is due to the MI spindle degradation delay that leads to a temporal coexistence of both MI and MII spindles in the cell. On the right, dot plot comparison of the time (min) between the start of spindle nucleation in meiosis I and meiosis II (SI-SII time) in h90 wild-type (wt; n = 30) versus h90 imp1Δ (n = 30) zygotic cells. p value was calculated using Student's *t* test (p value ns).

(B) Schematic set up of spindle dynamics in h90 wild-type (wt) vs. h90 imp1Δ zygotic cells at meiosis I and meiosis II from Figure 1A data. "IK" represents the interkinesis period whereas "overlap" represents the time of coexistence of MI and MII spindle.

(C) Time-lapse microscopy images of h90 wt and h90 imp1Δ zygotic cells (dotted white lines) expressing mCherry-Atb2 (microtubule marker), Sid2-Tomato (SPB) and Ndc80-GFP (kinetochores) throughout MI and MII. Normal genome segregation (wt control) and uneven segregation of sister chromatids during MII (white

Figure 1. Continued

arrows) with chromosome retention at MII onset (blue arrows) in imp1Δ backgrounds are shown. Numbers on top represent time in minutes. On the right, enlarged images highlight the mentioned stages of meiosis progression (metaphase II (84 min) and anaphase II (96 min)). Scale bar = 5μm.

(D) Time-lapse microscopy images of h90 wt and h90 imp1Δ zygotic cells (dotted white lines) expressing mCherry-Atb2 (microtubule marker), Sid2-Tomato (SPB) and Mis6-GFP (kinetochores) throughout MI and MII. Normal genome segregation (wt control) and uneven segregation of sister chromatids during MII with chromosome retention at MII onset (white arrows) in imp1Δ backgrounds are shown. Numbers on top represent time in minutes. On the right, enlarged image highlighting the referred stage of meiosis progression (metaphase II; 72 min). Scale bar = 5μm.

(E) Time-lapse microscopy images of h90 wt and h90 imp1Δ zygotic cells (dotted white lines) expressing mCherry-Atb2 (microtubule marker), Sid2-Tomato (SPB) and CENII-lacO lacI-GFP (centromere II) throughout MII. Normal genome segregation (wt control) and uneven segregation of sister chromatids during MII (white arrows) with chromosome retention at MII onset (blue arrows) in imp1Δ backgrounds are shown. Remanent MI spindle during MII is indicated (asterisk). Numbers at the top represent time in minutes. On the right, enlarged image highlights the mentioned stage of meiosis progression (anaphase II, 24 min). Scale bar = 5μm.

(F) Time-lapse microscopy images of h90 wt and h90 imp1Δ zygotic cells (dotted white lines) expressing mCherry-Atb2 (microtubule marker), Sid2-Tomato (SPB) and CENII-lacO lacI-GFP (centromere II) throughout MII. MI spindle persistence in imp1Δ zygotic cells leads to the retention of chromosomes near the old SPBs (blue arrows), resulting in the appearance of lagging chromosomes (white arrows). Scale bar = 5μm. On the center, percentage of MII nuclei (n = 88) with centromere II (CENII) retained near the old SPB (the one attached to the MI spindle; dark gray), the new SPB (the one not attached to the MI spindle; black) or with no retention (wild-type-like; light gray). Segregation pattern of CENII was assessed in time-lapse fluorescence microscopy of h90 imp1Δ zygotic cells with a fluorescent tagging at CENII (lacO insertions and expression of LacI-GFP). Retention phenotype was defined as meiosis II nuclei in which CENII is localized near one of the SPBs at prometaphase II for more than 5 min. On the right, percentage of meiosis II nuclei with CENII segregation defects in meiosis II of h90 wt (n = 136) and h90 imp1Δ (n = 189) zygotic cells. Lagging chromosomes (black) were defined as meiosis II nuclei in which at least one CENII dot does not colocalize with SPBs during anaphase II. Chromosome missegregation (gray) was defined as meiosis II nuclei in which a CENII signal is observed on a single SPB during anaphase II.

Aurora B from the spindle midzone to kinetochores is required to reset KtMT-kinetocore arrangements at the MI-MII transition, a key step to ensure accurate chromosome segregation during the two consecutive meiotic divisions in the absence of an intervening S phase.

RESULTS

Delayed meiosis I spindle disassembly is associated with chromosome segregation defects in meiosis II

By studying spindle dynamics in live fission yeast cells, we previously demonstrated that in mitosis, the importin α Imp1 is essential for triggering spindle disassembly in the spindle midzone at the end of anaphase.[18] During meiosis, we also determined that zygotes depleted for Imp1 delayed spindle disassembly in meiosis I, indicating that, as in mitosis, this importin α is also essential for spindle dissolution in meiosis I, but not in meiosis II, where spindle disassembly is triggered by the virtual Nuclear Envelope Breakdown (vNEBD).[17] Surprisingly, we observed that in this imp1Δ mutant background, MII spindles assembled even in the presence of persistent MI spindles, thus producing zygotic cells with coexisting MI and MII spindles. We observed that this property correlated with chromosome segregation defects in meiosis II,[17] suggesting that spindle coexistence may lead to MII chromosome missegregation.

To better understand the mechanism leading to MI-MII spindle cohabitation in zygotic cells and its relationship with chromosome missegregation events, we examined the dynamics of spindles, SPBs and chromosomes in individual living zygotes (see STAR Methods). As shown in Figure 1A, despite the extensive delay in MI spindle dissolution caused by the imp1Δ mutation, the MII spindle initiated assembly as in wt cells, with no significant delay after MI initiation. This observation suggests that spindle dynamics in MI and MII divisions are independent events programmed at the onset of meiosis,[19] resulting in frequent coexistence of MI and MII spindles when the timing of MI spindle dissolution overlaps with MII spindle assembly in imp1Δ zygotic cells, without affecting the total duration of meiosis II (see Figure 1B). More importantly, we confirmed that the coexistence of MI and MII spindles may cause chromosome segregation errors in MII (Figures 1C–1F and S1F), as previously suggested.[17]

Occasionally, tags used to mark kinetochore proteins may interfere with microtubule-kinetochore interactions. To discard tagging effects for this observation, we examined chromosome segregation related to spindle dynamics during meiosis using three independent kinetochore markers, the outer kinetochore protein Ndc80-GFP,[20] the p-lacO-lacI-GFP construct,[21] and the Mis6-GFP inner centromere marker.[22] As described above, persistent MI spindles in imp1Δ zygotes resulted in frequent lagging chromosomes and missegregation in meiosis II irrespective of the marker used (Figures 1C–1E and S1 and Video S1), indicating that proper disassembly of the MI spindle is required for the accurate segregation of sister chromatids in MII. Strikingly, we observed that in imp1Δ zygotic cells with coexisting MI and MII spindles, the non-segregating chromosomes in the second meiosis remained attached to the SPB that is still bound to MI spindle, referred here as the old SPB (Figure 1F). In Bub1-depleted budding yeasts, failure to correct initial meiotic attachments causes most chromosomes to travel to the old SPB.[23] Similarly, our results suggest that in these Imp1-depleted cells, the KtMTs-kinetochore arrays that segregated the homologous chromosomes likely persist into metaphase II.

Altered dynamics of spindle assembly checkpoint factors in Imp1-depleted zygotes

Such is the importance of proper assembly of spindle microtubules to sister kinetochores for accurate chromosome segregation, that eukaryotic cells have evolved a genetic pathway known as the spindle assembly checkpoint (SAC).[24] The SAC monitors the attachment of chromosomes to the spindle during metaphase, delaying the onset of anaphase until all chromosomes are properly attached and under tension.[25] This delay allows cells enough time to correct improper attachments, ensuring accurate chromosome segregation during mitosis[26] and in

Figure A

MTI duration (min) — schematic: Prophase I, Metaphase I, Anaphase I, Telophase I

MTII duration (min) — schematic: Prophase II, Metaphase II, Anaphase II, Telophase II

Legend: Spindle, SPB, Nucleous

MTI duration graph: imp1: + (30), Δ (37), + (18), Δ (13) mad2Δ, + (24), Δ (19) rec12Δ; comparisons ns, ns, ns

MTII duration graph: imp1: + (30), Δ (30), + (21), Δ (23) mad2Δ, + (30), Δ (22) clr4Δ; comparisons ns, ns, ****

B

MEIOSIS I — IK — MEIOSIS II

Wild type: 0, 10, 20, 30, 40, 50, 60, 70, 80, 90, 100, 110

Imp1Δ: 0, 10, 20, 30, 40, 50, 60, 70, 80, 90, 100, 110

Mad2-GFP   mCherry-Atb2
Sid2-Tomato

C

MEIOSIS I   MEIOSIS II

Legend: Spindle, SPB, Nucleous

PI, MT I, A I, IK, PII, MT II, A II

Fluorescence intensity (AU) vs Time (min)

wt, imp1Δ

D

Anaph. I   MT II

Wild type: 40, 60

imp1Δ: 60, 90

Ndc80-mTurq2   mCherry-Atb2
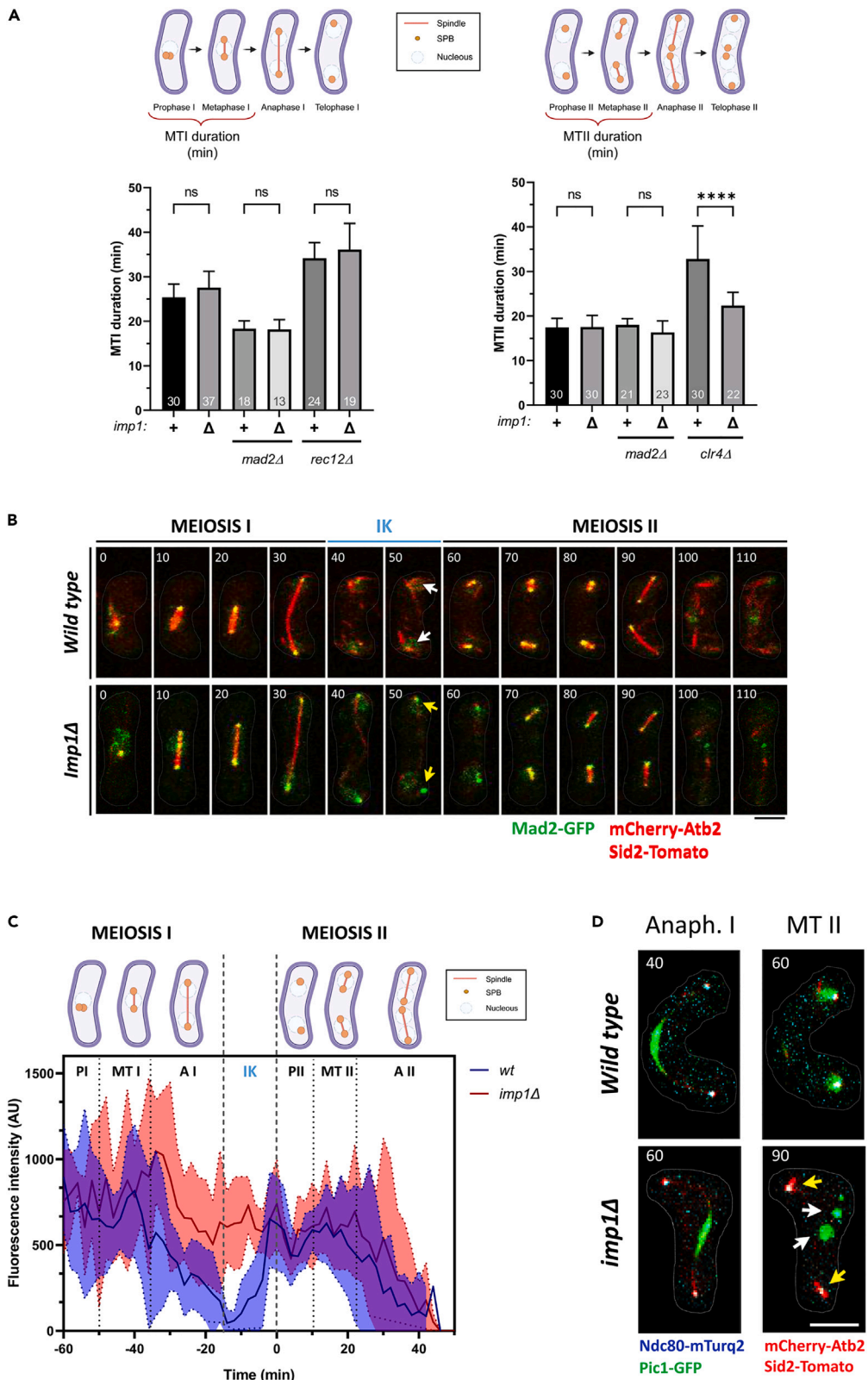Pic1-GFP   Sid2-Tomato

Figure 2. Mad2 and Aurora B/Ark1 kinase analysis during the meiotic cycle

(A) Duration of metaphase I (MTI; left) and duration of metaphase II (MTII; right) in minutes as considered in the above cartoons, corresponding to the phase I (initial spindle growth) and phase II (constant length) of spindle nucleation dynamics prior to spindle elongation at anaphase. The times were measured from zygotic cells analyzing the spindle (mCherry-atb2) and SPB (Sid2-Tomato) dynamics, in the control and mutant backgrounds indicated at the bottom. p values were calculated using non-parametric Kruskal-Wallis one-way ANOVA. Relevant significant (****p < 0.0001) and non-significant (ns) differences are indicated.

(B) Time-lapse microscopy images of h90 wt and h90 imp1Δ zygotic cells (dotted white lines) expressing mCherry-Atb2 (microtubule marker), Sid2-Tomato (SPBs) and Mad2-GFP throughout MI and MII. Normal Mad2 dynamics (white arrows) in wt control (upper panel) and abnormal persistence of Mad2 dots at interkinesis (IK; yellow arrows) in imp1Δ background with MI spindle disassembly delay (overlapping). Numbers on top represent time in minutes. Scale bar = 5μm.

(C) Mad2-GFP fluorescence intensity (AU) dynamics throughout meiosis I (PI: prophase I, MTI: metaphase I and AI: anaphase I) and meiosis II (PII: prophase II, MTII: metaphase II and AII: anaphase II) of h90 wt (blue; n = 6) and h90 imp1Δ (red; n = 6) zygotic cells. Average values (bold lines) and Standard Deviation (colored area) are indicated. Different meiotic stages are indicated within black dashed lines.

(D) Fluorescence images of the h90 wt and h90 imp1Δ cells (dashed white lines) expressing mCherry-Atb2 (microtubule marker), Sid2-Tomato (SPBs), Ndc80-mTurquiose2 (Centromeres) and Pic1-GFP (CPC) during anaphase I and metaphase II (MTII) (from Figure S4). Pic1-GFP re-localizes to both daughter nuclei in MII, but under persistent MI spindles, Pic1-GFP remains trapped at the spindle midzone (white arrows) decreasing its protein amount in the kinetochores of MII (yellow arrows). Scale bar = 5μm.

both meiotic divisions.[27,28] Thus, the duration of metaphase-to-anaphase transition (referred here as metaphase duration) can be used as a readout of SAC activation.[19,29]

To investigate whether persistent MI spindles found in Imp1-depleted zygotes could led to MII chromosome missegregation by interfering proper KtMT-kinetochore attachments, we analyzed SAC activation. To this end, we first determined the metaphase duration at MI and MII in imp1Δ as compared to wild-type (wt), and in different genetic backgrounds to either inactivate SAC (mad2Δ) or activate it specifically in meiosis I (rec12Δ) or meiosis II (clr4Δ) respectively.

In rec12Δ mutants, chromosomes bind to the spindle incorrectly due to the lack of chiasmata and therefore SAC delays the onset of anaphase in MI.[29] As shown in Figures 1C and 1D, both wt and imp1Δ strains segregate homologous chromosomes accurately in meiosis I. Both strains show also similar timing for anaphase I initiation and the rec12Δ mutation delays anaphase onset in both strains in a similar fashion (see in Figure 2A, left panel). Depletion of Mad2 (mad2Δ backgrounds), which abolishes SAC function,[10] rendered also similar metaphase duration in imp1Δ and in wild-type cells. These results indicate that SAC signaling is fully functional during MI in imp1Δ as in wt zygotic cells.

Using the clr4Δ mutation, in which SAC specifically delays anaphase initiation in meiosis II,[19,30] we forced SAC activation at this stage in wt and imp1Δ backgrounds. As expected, chromosome and spindle dynamics show that the clr4Δ-mediated SAC activation delays anaphase II onset in the wt background cells. However, this delay was poor in the imp1Δ clr4Δ double mutant indicating that the SAC, despite evident KT missegregation (see in Figure 1), is not fully active during MII in zygotes depleted for Imp1. In fact, metaphase duration in imp1Δ clr4Δ zygotes is similar to that observed in imp1Δ mad2Δ zygotes (Figure 2A, right panel), suggesting that the SAC is not properly signaling the errors leading to chromosome missegregations observed in imp1Δ cells. Among all known components of SAC complex, Mad2 is at the bottom and Aurora B kinase (Ark1) at the top of the kinetochore localization hierarchy.[31] To obtain clues about the molecular bases of the SAC malfunction in Imp1-depleted cells, we next investigated the localization of these two key elements along the meiotic cycle.

Mad2 is one of the best-characterized SAC factors.[25] Binding of this protein is stimulated by kinetochores that fail to attach to the spindle or to generate tension, in order to delay anaphase onset by directly inhibiting the APC/C Cdc20 activity.[32] Mad2-GFP localization was examined in living zygotes and its amount quantified by GFP fluorescence intensities during meiotic progression. In wild-type control cells, Mad2-GFP localizes at kinetochores in metaphase I until late anaphase I and delocalizes at the MI-MII transition (interkinesis). This SAC factor is recruited again in pro-metaphase II to the kinetochores until sister chromatids successfully segregate in anaphase II. However, in imp1Δ zygotes, an important fraction of Mad2-GFP remains at kinetochores during the MI-MII transition (Figures 2B and 2C). The persistence of Mad2-GFP at the kinetochores, together with the previous observation that chromosomes remain attached to the old SPB at the MII anaphase onset (see Figure 1F), suggest that syntelic KtMT-kinetochores arrangements required for homologs segregation are not resolved during the MI-MII meiotic window in this mutant.

Spindle midzone-kinetochore re-localization of the Aurora B-chromosomal passenger complex complex at the meiosis I-meiosis II transition

In mitosis, Aurora B plays a well-established role in correcting erroneous KtMT-kinetochore attachments during the SAC response.[33–35] Loss of Aurora B in budding yeast (Ipl1) or fission yeast (Ark1) meiosis leads to massive chromosome missegregation due to the failure to correct initial erroneous attachments.[9,36–38] Aurora B forms a stable complex with INCENP (the Ark1-Pic1 complex in S. pombe), and together with borealin (Nbl1) and survivin (Bir1), constitutes the conserved chromosomal passenger complex (CPC). The CPC localizes to various regions at different times during mitosis, where the enzymatic subunit, Aurora B kinase, regulates key mitotic events.[39] In S. pombe mitosis, Aurora B-CPC does not associate with the SPB/kinetochore complex in interphase. However, following mitotic commitment, Ark1 concentrates particularly on prometaphase-metaphase kinetochores. During anaphase, Ark1 distributes along the spindle, and it gets restricted to the midzone as the spindle extends.[40] To assess Aurora B-CPC localization dynamics in wt and imp1Δ meiosis, we visualized Ark1-GFP but also other three GFP-tagged CPC components (Pic1, Nbl1, Bir1). All four proteins followed identical localization dynamics in the progression of meiosis

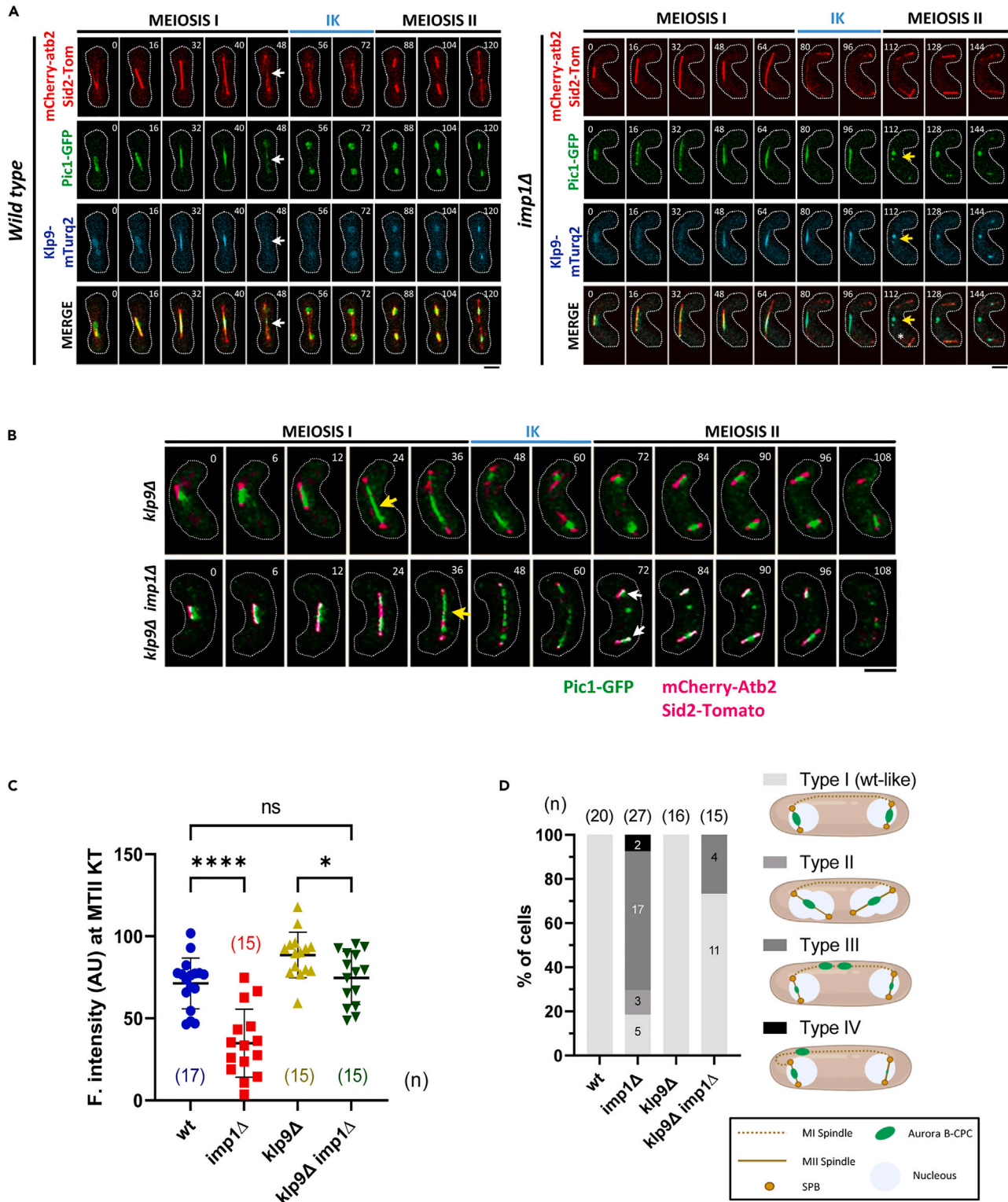**Figure 3. Kinesin-6 klp9 deletion (klp9Δ) restores Aurora B-CPC spindle midzone to kinetochore re-localization at interkinesis**

(A) Time-lapse fluorescence images of a representative h90 wt cell (left panel) and h90 imp1Δ cell (right panel) expressing mCherry-Atb2 (microtubule), Sid2-Tomato (SPBs), Pic1-GFP (CPC), and klp9-mTurquoise2. Remanent MI spindle during MII is indicated by asterisks. Normal midzone disassembly (wt control)

Figure 3. Continued

with Klp9-mTurq2 and Pic1-GFP foci disappearance (white arrows) and abnormal Klp9-mTurq2 and Pic1-GFP persistence at MII onset (yellow arrows) in imp1Δ backgrounds are shown. Numbers at the top represent time in minutes. Scale bar = 5 μm.

(B) Time-lapse fluorescence images of a representative h90 klp9Δ cell (top panel) and h90 klp9Δ imp1Δ cell (bottom panel) expressing mCherry-Atb2 (microtubule), Sid2-Tomato (SPBs), and Pic1-GFP (CPC). Pic1 localizes to the entire anaphase I spindle (yellow arrows). The lack of Klp9 allows its re-localization at prometaphase II nuclei (white arrows) even in the absence of imp1. Numbers at the top represent time in minutes. Scale bar = 5 μm.

(C) Fluorescence intensity quantification (AU) of Aurora B-CPC (Pic1-GFP) at metaphase II kinetochores in h90 wt (n = 17), h90 imp1Δ (n = 15), h90 klp9Δ (n = 15), and h90 klp9Δ imp1Δ (n = 15) zygotic cells. p values were calculated using an ordinary one-way ANOVA. Statistically significant (*p < 0.05; ****p < 0.0001) and non-significant (ns) differences are indicated (n ≥ 15).

(D) Percentage of h90 wt (n = 20), h90 imp1Δ (n = 27), h90 klp9Δ (n = 16), and h90 klp9Δ imp1Δ (n = 15) zygotic cells with the different types of Aurora B-CPC re-localization phenotypes that we appreciate (classified into Type I-IV drawn in Cartoons on the right; see also Figure S3).

(Figure S2). To avoid any potential tagging-related interference with Ark1 enzymatic functions, we followed Pic1-GFP/INCENP constructs to analyze Aurora B/Ark1 localization thought the Ark1-Pic1-GFP complex.[41,42]

By analyzing the Ark1-Pic1-GFP complex, we observed that during MI, Aurora B-CPC accumulates at kinetochores from prophase to the onset of anaphase I, when this kinase redistributes to the spindle midzone during spindle elongation, similar to its localization during mitosis (Figures 2D upper panels and S2).[40,43–45] Midzone-associated Aurora B-CPC is then released upon spindle disassembly at the exit of meiosis I. Importantly, in the absence of an intervening S phase, released Ark1/CPC from the MI spindle midzone directly targets the kinetochores during the MI-MII transition (Figures 2D upper panels and S2).

As compared to wild-type, imp1Δ zygotes delay spindle midzone disassembly at MI, which often remains assembled as the zygote enters MII (Figure 1B).[17] Remarkably, in these imp1Δ zygotes, Aurora B-CPC remains trapped at the persistent midzone during the MI-MII transition and enters MII with poor or undetectable Aurora B-CPC signal at kinetochores (Figures 3A, S2, S3A, and S3B). Since kinetochore localization of Aurora B kinase is required for error-correction activity at KtMT-kinetochore arrays and full SAC signaling in mitosis,[11,46] we hypothesize that sequestered Aurora B at the spindle midzone during the MI-MII transition hinders KtMT-kinetochore corrections and proper SAC action at the MII onset in imp1Δ cells (Figure 2A), resulting in lagging and chromatids missegregation during anaphase II (Figures 1C–1F and S1).

Ectopic release of the midzone-trapped Aurora B-chromosomal passenger complex restores its kinetochore re-localization in Imp1-depleted zygotes

It has been described that Aurora B association with the spindle midzone in mitosis is dependent on Kinesin-6,[47,48] the Klp9 protein in fission yeast.[49,50] Accordingly, Pic1-GFP co-localizes with Klp9-GFP in the spindle midzone during anaphase I in S. pombe wild-type zygotes, and both proteins remain associated to the midzone until disassembly, at which point Aurora B-Pic1-GFP is found to relocate to MII centromeres (Figures 3A left and S2). Accordingly, in Imp1-depleted zygotes both proteins remain attached to the persistent MI spindle midzone, a small or no signal of Klp9 nor Pic1 being detected at kinetochores during the MI-MII transition (Figures 3A right and S2). Importantly, Klp9 depletion (klp9Δ mutant) reduces CPC accumulation in the midzone (even though the spindle I remains assembled), significantly restoring its kinetochore localization (Figures 3B and 3C) and a wt-like dynamics of the Aurora B complex at the MI-MII transition in imp1Δ cells (Figures 3B and 3D). We identified up to three abnormal phenotypical classes of Ark1-Pic1 localization defects with different frequencies in imp1Δ mutant zygotes (cartoon in Figures 3D and S3), most of them being efficiently suppressed by Klp9 depletion (Figure 3D).

Ase1 protein stabilizes interdigital spindle midzone. Lack of this protein lead to weaker and fragile spindles that randomly break down prematurely while elongating.[51–53] Accordingly, ase1Δ supresses hyperelongated spindles at mitosis in imp1Δ cells.[18] Interestingly, imp1Δ ase1Δ cells that break up the spindle before the interkinesis free up the Aurora B-CPC complex from the spindle midzone and, as described for Klp9 depletion, imp1Δ ase1Δ zigotes significantly restores wt-like localization dynamics of Aurora B-Pic1-GFP at the MI-MII transition (Figures S6B and S6C).

Thus, release of midzone-trapped Aurora B-CPC in imp1Δ, either directly through Klp9 depletion or indirectly by premature spindle dissolution in the ase1Δ mutant background, re-establishes its kinetochore localization during interkinesis.

Released Aurora B-chromosomal passenger complex restores normal chromosome MII segregation and spindle assembly checkpoint function in Imp1-depleted zygotes

To determine whether midzone-sequestered Aurora B in persistent MI spindles leads to MII chromatid segregation errors, we studied spindle and chromosome dynamics in imp1Δ zygotic cells depleted for the Klp9 Kinesin-6 along with respective controls. While the depletion of Klp9 have not a significant impact on the delay of MI spindle disassembly compared to imp1Δ zygotes (Figure S5A), lack of Klp9 suppresses chromosome segregation errors at meiosis II in imp1Δ zygotes (Figure 4A). MI and MII coexistent spindles can also be observed in imp1Δ klp9Δ zygotic cells. Thus, segregation errors in meiosis II are unlikely due to abnormal interpolar spindle persistence itself but to Aurora B-CPC sequestration far away from the MII kinetochores. Similar results were observed by using Ase1 depletion to release AuroraB-Pic1-GFP from the midzone (Figure 4B). Quantitative analysis of chromosome retention in older SPBs during the MI-MII transition and segregation errors at the beginning of anaphase II in imp1Δ zygotes reinforce this observation (Figures 4C, 4D, S5B, S6B, S6 and S6C). Furthermore, Ark1 release mediated by klp9 deletion significantly restores SAC function in metaphase II as well (Figure 4E). Thus, midzone-associated Aurora B-CPC release permits the zygote to erase monopolar arrays at kinetochores during the MI-MII transition, underlying a key step required to assembly sister KT-KtMT bioriented arrays and proper SAC function at the MII onset.
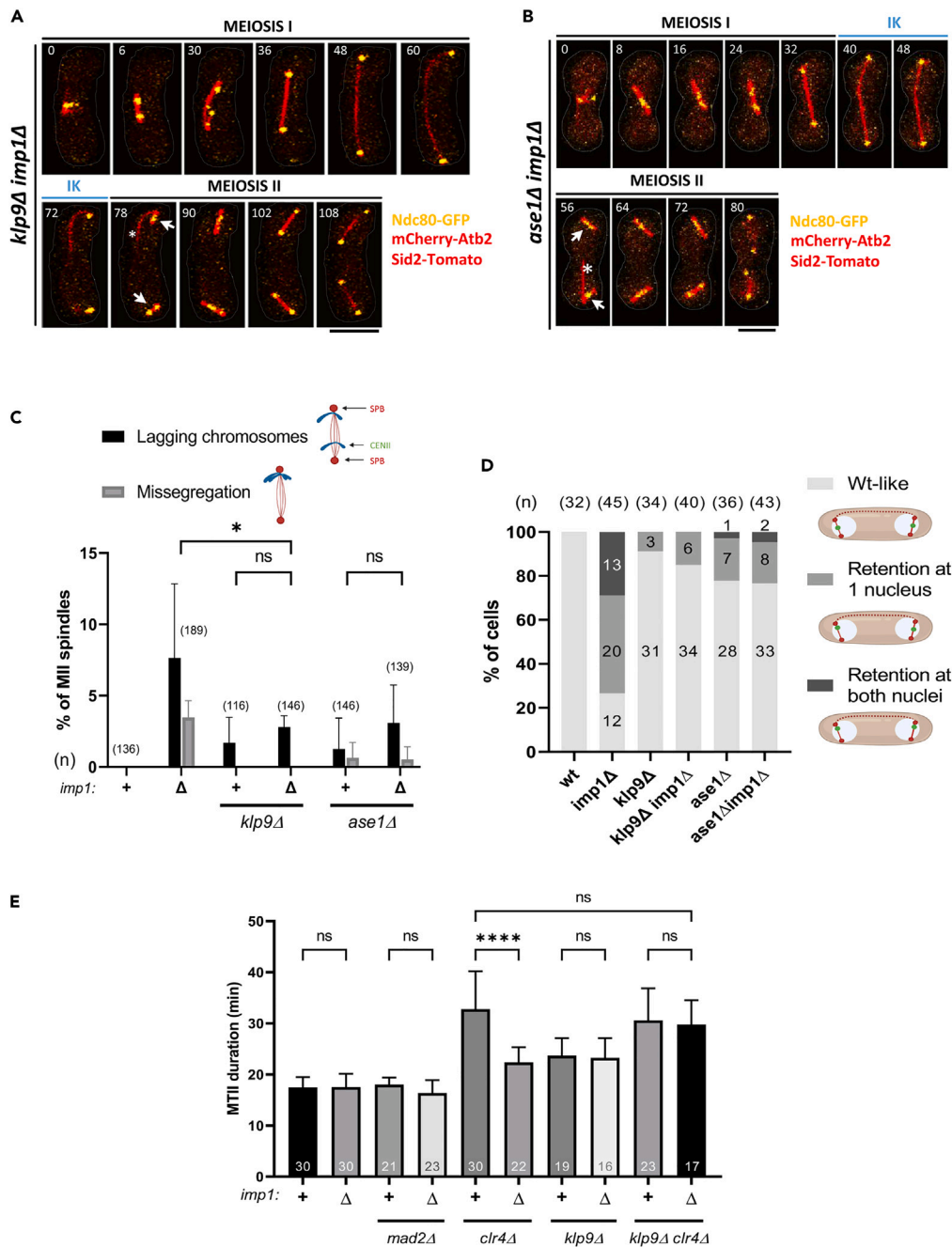
Figure 4. Deletion of Kinesin-6 klp9 or Ase1 restores sister chromosome segregation in imp1Δ meiosis II

(A) Time-lapse fluorescence images of a representative h90 klp9Δ imp1Δ cell expressing mCherry-Atb2 (microtubule), Sid2-Tomato (SPBs), and Ndc80-GFP (kinetochores). Remnant MI spindle during MII is indicated by asterisks. Normal segregation of sister kinetochores during MII with no chromosome retention at MII onset (white arrows) in klp9Δ imp1Δ backgrounds is shown. Numbers on top represent time in minutes. Scale bar = 5 μm.

(B) Time-lapse fluorescence images of a representative h90 ase1Δ imp1Δ cell expressing mCherry-Atb2 (microtubule), Sid2-Tomato (SPBs), and Ndc80-GFP (kinetochores). Remnant MI spindle during MII is indicated (asterisks). Normal genome segregation of sister chromatids during MII with no chromosome retention at MII onset (white arrows) in ase1Δ imp1Δ backgrounds is shown. Numbers at the top represent time in minutes. Scale bar = 5 μm.

(C) Quantification of meiosis II nuclei with CENII segregation defects in meiosis II. Segregation pattern of centromere II was assessed in time-lapse fluorescence microscopy of h90 wt (n = 136), h90 imp1Δ (n = 189), h90 klp9Δ (n = 116), h90 klp9Δ imp1Δ (n = 146), h90 ase1Δ (n = 146) and h90 ase1Δ imp1Δ (n = 139) cells as before. Lagging chromosomes (black) and Chromosome missegregation (gray) was defined as previously described (see upper cartoon). p values were calculated using Chi-square test. Relevant significant (*p < 0.05) and non-significant (ns) differences are indicated.

Figure 4. *Continued*

(D) Quantification of h90 wt (n = 32), h90 imp1Δ (n = 45), h90 klp9Δ (n = 34), h90 klp9Δ imp1Δ (n = 40), h90 ase1Δ (n = 36), h90 ase1Δ imp1Δ (n = 43) zygotic cells with chromosomes (CENII) retained near one of the two MII SPBs at MII onset at one nucleus (dark gray), both nuclei (black) or with no chromosome retention (wt-like; light gray). Segregation pattern of centromere II (CENII) was assessed in time-lapse fluorescence microscopy of h90 zygotic cells. Retention phenotype was defined as meiosis II nuclei in which centromere II is localized near one of the SPBs at prometaphase II for more than 5 min since MII spindle nucleation onset (see upper cartoon).

(E) Duration of metaphase II (MTII) in minutes as previously shown in Figure 2A but including klp9Δ and klp9Δ imp1Δ mutant backgrounds as indicated at the bottom. p values were calculated using non-parametric Kruskal-Wallis one-way ANOVA. Relevant significant (****p < 0.0001) and non-significant (ns) differences are indicated.

Similarly to the *imp1Δ* mutation, the deletion of the cytoplasmic microtubule organizer Mto1 (*mto1Δ*) leads to hyper-elongated meiosis I spindles,[54] often resulting in the coexistence of both meiosis I and meiosis II spindles (Figures S7A–S7C). However, *imp1Δ and mto1Δ* mutants lead to hyper-elongated spindles by independent mechanisms. Imp1 is required to initiate midzone spindle disassembly at MI,[17] while cells lacking Mto1 exhibit catastrophe defects leading to continuous spindle MTs growth.[54] This mutant leads to faulty karyogamy[55] and, in meiosis, it results in the extended duration of meiosis I but also meiosis II spindles (Figure S7C). Interestingly, by analyzing the fraction of zygotes undergoing karyogamy, we observe that, in the *mto1Δ* mutant, Pic1-GFP initiates its detachment from the midzone at the meiosis I spindle as in wild-type zygotes (Figures S8A–S8C). The *mto1Δ* mutant slows down microtubule depolymerization and the midzone remains for longer after disassembly is initiated (Figure S8B). Consequently, as indicated by the gradual recovery of *Pic1-GFP* signal in the nuclei at interkinesis (Figure S8B), midzone release of the Ark1-CPC signal also occurs slower than in the wild-type, yet more rapidly than in the *imp1Δ* mutant (Figure S8A, white arrows, and S8D). Nonetheless, albeit slower, Ark1-CPC relocation takes place in *mto1Δ* zygotes and importantly, this release allows chromosome segregation in MII. In this mutant, chromosomes are eventually trapped at the "old" SPB for a few minutes at the beginning of meiosis II (Figure S9A), but this entrapment is less frequent than that observed in *imp1Δ* mutants (Figure S9B) and ultimately, most chromosomes segregate correctly in anaphase II (Figure S9C). Consequently, the deletion of *mto1* does not result in significant segregation defects in meiosis II, suggesting that Aurora B-CPC midzone release, as midzone dissolution,[17,18] is Imp1-dependent.

Aurora B kinase activity is essential to reset meiosis I syntelic arrangements in the meiotic interkinesis

Since Aurora B kinase is the enzymatic partner of the quadripartite chromosome passenger complex, we asked whether suppression of chromosome missegregation upon midzone spindle release requires its enzymatic activity, or just physical assembly of CPC at meiosis II kinetochores. To answer this question, we reproduced CPC ectopic release experiments in strains harboring a conditional ATP analog-sensitive allele of Aurora B (*ark1.as3*), a mutation that renders kinase-dead activity in the presence of an ATP analog (1NM-PP1).[36,56] Ark1 is essential for faithful chromosome segregation both in meiosis I[36] and meiosis II.[57] To analyze the role of Ark1 kinase activity exclusively in meiosis II, time-lapse images of *ark1.as3* zygotes in the desired genetic backgrounds were taken until the completion of meiosis, and only cells that had just completed meiosis I before drug addition (1NM-PP1) were analyzed (Figure 5A). As previously reported, the inhibition of *ark1.as3* kinase at the MI-MII transition leads to massive segregation defects during meiosis II in wt background zygotes[57] (Figure 5B). Interestingly, the frequency of missegregating chromosomes that remain attached to the old SPB during anaphase II when inhibiting Aurora B activity at the MI-MII transition is remarkable (Figure 5B). This observation suggest that Aurora B kinase plays a central role in the disassembly of meiosis I KtMT-Kinetochrore arrays, to allow normal KtMT-Kinetochrore assembly at meiosis II. This frequency is enhanced in *imp1Δ* zygotes (*ark1.as3 imp1Δ* strain) in which, in addition to kinase inactivation, midzone-trapped CPC complex prevents normal Aurora B re-localization at the kinetochores. Furthermore, when *ark1.as3* is inhibited in the *imp1Δ klp9Δ* genetic background (*ark1.as3 imp1Δ klp9Δ* strain), chromosome missegregation is no longer suppressed despite the CPC ectopic release caused by the *klp9Δ* mutation (Figure 5B). The frequency of nuclei with missegregating chromosomes entrapment at the old SPB is near 60% in Imp1-depleted cells, but the inactivation of Ark1 in *ark1.as3 imp1Δ* zygotic cells raises this frequency to more than 90%, independently of the presence or not of Klp9 (94.11% in the *ark1.as3 imp1Δ klp9Δ* strain) (Figure 5C). Thus, we conclude that kinetochore's localization of kinase-active Ark1 is required to erase MI syntelic KtMT-KT interactions in the meiotic interkinesis for accurate sister chromatids segregation during meiosis II.

DISCUSSION

Meiosis I is a unique type of cell division that allows halving of the chromosome number. In contrast to mitosis, or meiosis II, sister kinetochores attach to microtubules from the same pole (mono-orientation) during meiosis I. Aurora B controls sister chromatids mono-orientation and homologous chromosome biorientation.[27,36] Chiasmata that pair homologous chromosomes plays a key role in this process. In fission yeast, the biorientation of fused sister kinetochores (amphitelic arrays as in mitosis) predominates during early prometaphase I, but after chiasmata connection, homolog chromosome kinetochores are arranged to the outer edge, re-positioning Aurora B inward.[29] This repositioning favors Aurora B to stabilize homologous chromosome biorientation over that of sister chromatids, and mono-orientate syntelic arrays at sister chromatids are stabilized.[29] Once the SAC is satisfied, the onset of anaphase I is triggered and, as in mitosis,[39,40] Aurora B re-localizes from centromeres in metaphase I to the spindle midzone in anaphase I (see in Figures 3A and S1).

During meiosis II, chromatids are segregated as in mitosis, and bioriented amphitelic attachments are required at sister kinetochores to undergo equational segregation.[28] A requirement for faithful chromosome segregation is establishing proper attachments between chromosomes and spindle microtubules.[16] Accordingly, stabilized syntelic attachments of sister kinetochores in meiosis I require correction before
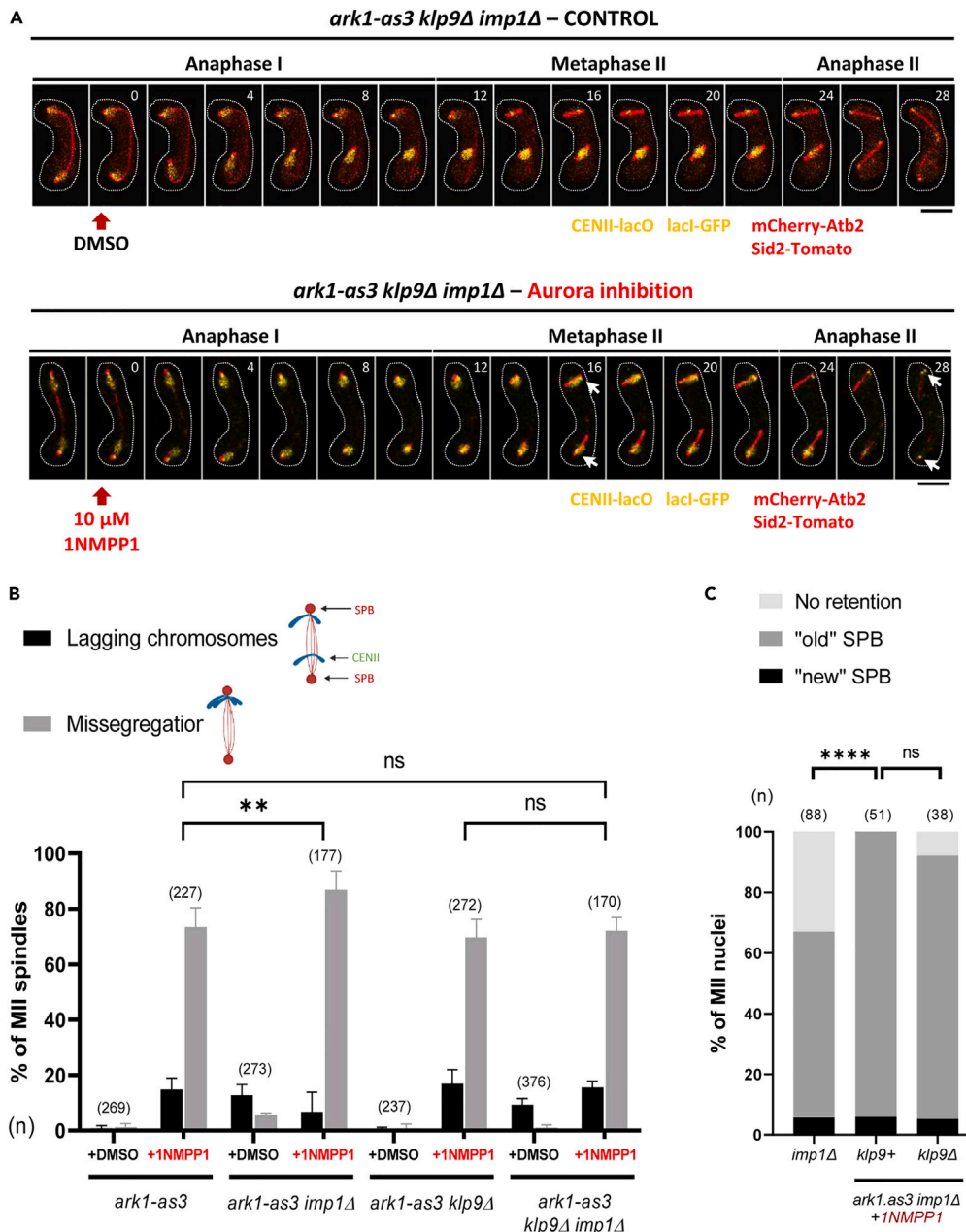
Figure 5. Aurora B kinase is required for proper kinetochore to spindle microtubules attachments during meiosis II

(A) Time-lapse fluorescence images of a representative h90 ark1-as3 klp9Δ imp1Δ cell in the absence (only DMSO solvent; upper panel) or presence of inhibitor (10 μM of 1NMPP1) (right panel) expressing mCherry-Atb2 (microtubule), Sid2-Tomato (SPBs) and CENII-lacO LacI-GFP (centromere II). Normal sister chromatids segregation during MII in the absence of inhibitor and uneven segregation of sister chromatids during MII (white arrows) in the presence of inhibitor are shown. Numbers at the top indicate time in minutes. Red arrows indicate the time of DMSO or 1NMPP1 addition to the medium. Scale bar = 5 μm.

(B) Percentage of meiosis II nuclei with CENII segregation defects in ATP analog-sensitive Aurora allele backgrounds (ark1-as3 and double ark1-as3 imp1 Δ). The absence (only DMSO solvent) or the presence of inhibitor (10 μM of 1NMPP1) determines the kinase active or dead state of Aurora. Segregation pattern of CENII was assessed in time-lapse fluorescence microscopy of h90 ark1-as3 + DMSO (n = 269), h90 ark1-as3 + 1NMPP1 (n = 224), h90 ark1-as3 imp1Δ + DMSO (n = 228), h90 ark1-as3 imp1Δ + 1NMPP1 (n = 162), h90 ark1-as3 klp9Δ + DMSO (n = 376) and h90 ark1-as3 klp9Δ imp1Δ + 1NMPP1 (n = 170), with a fluorescent tagging at CENII (lacO insertions plus LacI-GFP expression). Lagging chromosomes (black) were defined as meiosis II nuclei in which at least one CENII does not colocalize with SPBs during anaphase II. Chromosome missegregation (gray) was defined as meiosis II nuclei in which a CENII signal is observed on a single SPB during anaphase II. p values were calculated using Chi-square test. Relevant significant difference (**p < 0.01) is indicated.

(C) Percentage of MII nuclei in h90 imp1Δ zygotic cells (n = 88), h90 ark1.as3 imp1Δ +10 μM of 1NMPP1 (n = 51), and h90 ark1.as3 klp9Δ imp1Δ +10 μM of 1NMPP1 (n = 38) with centromere II (CENII) retained near the old SPB (the one attached to the MI spindle; dark gray), the new SPB (the one not attached to the MI spindle;

Figure 5. *Continued*

black) or with no retention (wild-type-like; light gray). The segregation pattern of CENII was analyzed using time-lapse fluorescence microscopy of h90 zygotic cells with a fluorescent marker on CENII (lacO insertions and expression of LacI-GFP). The chromosome retention phenotype was defined as MII nuclei in which the CENII dots remained close to one of the SPBs in prometaphase II for more than 5 min. p values were calculated using Chi-square test. Relevant significant (****p < 0.0001) and non-significant (ns) differences are indicated.

meiosis II onset to propitiate amphitelic arrays at this second meiotic division. We report here that in the absence of Aurora B activity at kinetochores during the MI-MII window -as observed in *imp1Δ* zygotes with midzone-sequestered Ark1 and through the chemical inactivation of *ark1-as* mutants- MI syntelic attachments remain stabilized and kinetochores remain attached to the old SPB at the onset of MII (Figure 1E). Consistently, we also observed a significant amount of Mad2 over the interkinesis that may be signaling this abnormality (Figure 2C). These uncorrected kinetochore arrays likely maintain normal numbers of microtubules,[58] diminishing the formation of new attachments from the MII spindle which eventually, joined to a deficient SAC signaling (Figure 2C), lead to lagging chromosomes and missegregation during anaphase II (see in Figures 1B and 1C). Releasing midzone-trapped Aurora B-CPC complexes in *imp1Δ* zygotes, either by Klp9-depletion (Figure 3) or by premature spindle dissolution in *ase1Δ* mutant backgrounds (Figure S6), restore a wt-like dynamics of Aurora B-CPC and crucially, significantly suppress segregation errors at meiosis II (Figure 4). Therefore, the error-correction activity of Aurora B functions at the meiotic interkinesis to erase MI monopolar arrays prior meiosis II onset, a key step required to ensure accurate segregation during meiosis II.

Interestingly, we observed that SAC response in meiosis II is also defective in the *imp1Δ* mutant (Figure 2A). Since displacing Ark1 from the mid-spindle by genetic means (*klp9Δ*) fully restores meiosis II SAC function in this strain (Figure 4E), we conclude that Aurora B re-localization from MI mid-spindle to kinetochores at the MI-MII transition is also required to create SAC-proficient kinetochores and full SAC signaling at MII. In contrast, SAC function analysis indicates that *imp1Δ* zygotes are not deficient in this pathway during meiosis I (Figure 2A). However, as previously described in budding yeasts,[59] we noted that the normal metaphase I duration is reduced by 30% in Mad2-depleted zygotes both in wt and *imp1Δ* zygotes (Figure 2A), suggesting that the SAC is delaying normal MI progression even in the absence of any insult. This delay is not observed in mitosis nor in meiosis II (ref.[57] and Figure 1A, right panel). This extra time provided by the SAC at meiosis I is likely required to resolve chiasmata and/or to assemble the unique KtMT-KT arrays required to segregate homologous chromosomes.[29]

As compared to the mitotic division cycle, different adaptive mechanisms evolved to produce haploid gametes from diploid cells by two consecutive meiotic divisions. To avoid S phase, studies in frogs have shown that Anaphase Promoting Complex/Cyclosome (APC/C) does not fully degrade cyclin at the end of the first division, as in mitosis, thus maintaining Cdk activity at an intermediate level at the MI-MII transition and allowing MII initiation without DNA replication.[60] During segregation, chromosomes are bound by the cohesin complex until one of its proteins is degraded via APC/C at the metaphase I-to-anaphase I transition; but pericentromeric cohesin must be protected from cleavage in meiosis I until the segregation of MII chromatids.[61,62] Similarly, in the absence of interphase, meiotic kinetochores remain assembled in condensed chromosomes at the MI-MII transition,[13] as evidenced by the localization of Ndc80 (Figure 1C). It has been reported in mouse oocytes that Aurora-B/C-dependent "error-correction" as well as SAC activation take place upon the reduction of tension applied by the spindle on correctly bioriented bivalents in late prometaphase I.[63] Here we show by first time that the "error-correction" activity of Aurora B also targets syntelic kMT-kinetochore arrays of segregating homologs at the MI-MII transition, after these arrays were stabilized in prometaphase and homologs segregation licensed by the SAC.

Overall, we propose that this late anaphase I activity of Aurora B plays a pivotal role in the physiological disassembly of syntelic kMT-kinetochore arrays at anaphase I exit, a step that become essential to execute consecutive reductional and equational divisions in the absence of an intervening interphase (Figure 6). Moreover, because Aurora B recruitment to MII kinetochores depends on its prior release as the spindle I disassembles, Aurora B relocation may be a key step licensing meiosis II onset after successful anaphase I segregation (see schematic model in Figure 6). Remarkably, our results suggest that Aurora B-CDC midzone release likely depends on Imp1 function (Figures S7–S9), either by the same mechanism employed for initiating spindle midzone disassembly,[17,18] and/or by a more direct function.[18]

In human meiosis, chromosome missegregation occur at both MI and MII.[64] The finding described here may also provide evidence for an additional source of human chromosome mis-segregations of clinical relevance.

Limitations of the study

Aurora B re-localization to kinetochores after MI spindle midzone dissolution is a key step in resetting microtubule-kinetochore arrangement prior to the onset of MII. We show that this step depends on Imp1, but is not yet clear whether Imp1-triggered spindle dissolution releases Aurora B from the midzone, or whether Imp1 directly mediates Aurora B release in parallel to midzone disassembly (or both).

STAR★METHODS

Detailed methods are provided in the online version of this paper and include the following:

- KEY RESOURCES TABLE
- RESOURCE AVAILABILITY
  - Lead contact
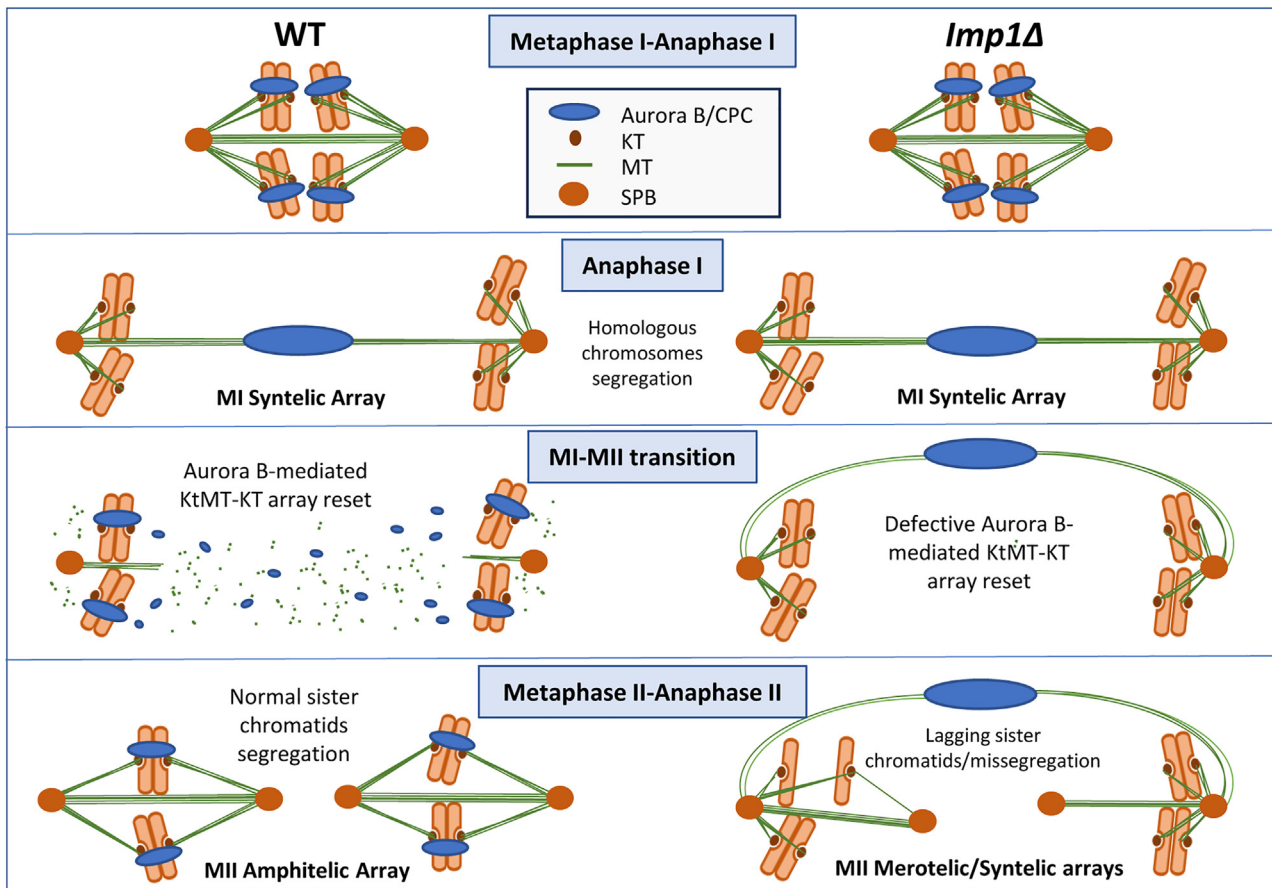 - Materials availability
  - Data and code availability

Figure 6. A model illustrating the key role of Aurora B at KtMT- Kinetochore arrangements reset at the MI-MII transition

Schematic model of the role of Aurora B-CPC (blue) in kinetochore to microtubules attachment remodeling at MI-MII transition in wild-type (left) and imp1Δ (right) meiosis. During prometaphase I, chromosomes (orange) connect to spindle microtubules (MT, green). Centrosomes (black circles) are the SPBs, the main microtubule-organizing centers of fission yeast cells. During MI, syntelically attached chromosome pairs are required for homologous segregation. These attachments are necessarily disassembled to permit MII amphitelic arrays, a reset mechanism driven by Aurora B kinase. Defective Aurora B-CPC re-localization in imp1Δ meiosis leads to chromosome missegregation at meiosis II due to the maintenance of syntelic attachment from MI and lagging chromosomes defects due to the formation of merotelic attachments at MII.

- EXPERIMENTAL MODEL AND STUDY PARTICIPANT DETAILS
  - *S. pombe* strains and culture
- METHOD DETAILS
  - Aurora B kinase inhibition assays
  - Live-cell microscopy
  - Image analysis and measurement of spindle and chromosome dynamics
- QUANTIFICATION AND STATISTICAL ANALYSIS
  - Quantification of fluorescent signals
  - Statistical analysis

SUPPLEMENTAL INFORMATION

Supplemental information can be found online at https://doi.org/10.1016/j.isci.2023.108339.

ACKNOWLEDGMENTS

AUTHOR CONTRIBUTIONS

S.V.-C., V.A.T. and J.J. designed the experiments. S.V.-C. performed the experiments and analyzed the data. VAT supervised. J.J. acquired funding and wrote the article with input from S.V.-C. and V.A.T.

DECLARATION OF INTERESTS

The authors declare no competing interests.

REFERENCES

1. Ding, R., McDonald, K.L., and McIntosh, J.R. (1993). Three-dimensional reconstruction and analysis of mitotic spindles from the yeast, Schizosaccharomyces pombe. J. Cell Biol. 120, 141–151. https://doi.org/10.1083/jcb.120.1.141.

2. Kirschner, M., and Mitchison, T. (1986). Beyond self-assembly: from microtubules to morphogenesis. Cell 45, 329–342. https://doi.org/10.1016/0092-8674(86)90318-1.

3. Mastronarde, D.N., McDonald, K.L., Ding, R., and McIntosh, J.R. (1993). Interpolar spindle microtubules in PTK cells. J. Cell Biol. 123, 1475–1489. https://doi.org/10.1083/jcb.123.6.1475.

4. Dong, Q., and Li, F. (2022). Cell cycle control of kinetochore assembly. Nucleus 13, 208–220. https://doi.org/10.1080/19491034.2022.2115246.

5. Goshima, G., Saitoh, S., and Yanagida, M. (1999). Proper metaphase spindle length is determined by centromere proteins Mis12 and Mis6 required for faithful chromosome segregation. Genes Dev. 13, 1664–1677. https://doi.org/10.1101/gad.13.13.1664.

6. Hayashi, A., Asakawa, H., Haraguchi, T., and Hiraoka, Y. (2006). Reconstruction of the kinetochore during meiosis in fission yeast Schizosaccharomyces pombe. Mol. Biol. Cell 17, 5173–5184. https://doi.org/10.1091/mbc.e06-05-0388.

7. Kerres, A., Vietmeier-Decker, C., Ortiz, J., Karig, I., Beuter, C., Hegemann, J., Lechner, J., and Fleig, U. (2004). The fission yeast kinetochore component Spc7 associates with the EB1 family member Mal3 and is required for kinetochore-spindle association. Mol. Biol. Cell 15, 5255–5267. https://doi.org/10.1091/mbc.e04-06-0443.

8. de Regt, A.K., Clark, C.J., Asbury, C.L., and Biggins, S. (2022). Tension can directly suppress Aurora B kinase-triggered release of kinetochore-microtubule attachments. Nat. Commun. 13, 2152. https://doi.org/10.1038/s41467-022-29542-8.

9. Monje-Casas, F., Prabhu, V.R., Lee, B.H., Boselli, M., and Amon, A. (2007). Kinetochore orientation during meiosis is controlled by Aurora B and the monopolin complex. Cell 128, 477–490. https://doi.org/10.1016/j.cell.2006.12.040.

10. Rieder, C.L., Cole, R.W., Khodjakov, A., and Sluder, G. (1995). The checkpoint delaying anaphase in response to chromosome monoorientation is mediated by an inhibitory signal produced by unattached kinetochores. J. Cell Biol. 130, 941–948. https://doi.org/10.1083/jcb.130.4.941.

11. Roy, B., Han, S.J.Y., Fontan, A.N., Jema, S., and Joglekar, A.P. (2022). Aurora B phosphorylates Bub1 to promote spindle assembly checkpoint signaling. Curr. Biol. 32, 237–247.e6. https://doi.org/10.1016/j.cub.2021.10.049.

12. Lampson, M.A., Renduchitala, K., Khodjakov, A., and Kapoor, T.M. (2004). Correcting improper chromosome-spindle attachments during cell division. Nat. Cell Biol. 6, 232–237. https://doi.org/10.1038/ncb1102.

13. Sato, M., Kakui, Y., and Toya, M. (2021). Tell the Difference Between Mitosis and Meiosis: Interplay Between Chromosomes, Cytoskeleton, and Cell Cycle Regulation. Front. Cell Dev. Biol. 9, 660322. https://doi.org/10.3389/fcell.2021.660322.

14. Zhang, R., Liu, Y., and Gao, J. (2023). Phase separation in controlling meiotic chromosome dynamics. Curr. Top. Dev. Biol. 151, 69–90. https://doi.org/10.1016/bs.ctdb.2022.04.004.

15. Yokobayashi, S., and Watanabe, Y. (2005). The kinetochore protein Moa1 enables cohesion-mediated monopolar attachment at meiosis I. Cell 123, 803–817. https://doi.org/10.1016/j.cell.2005.09.013.

16. Cairo, G., and Lacefield, S. (2020). Establishing correct kinetochore-microtubule attachments in mitosis and meiosis. Essays Biochem. 64, 277–287. https://doi.org/10.1042/ebc20190072.

17. Flor-Parra, I., Iglesias-Romero, A.B., Salas-Pino, S., Lucena, R., Jimenez, J., and Daga, R.R. (2018). Importin α and vNEBD Control Meiotic Spindle Disassembly in Fission Yeast. Cell Rep. 23, 933–941. https://doi.org/10.1016/j.celrep.2018.03.073.

18. Lucena, R., Dephoure, N., Gygi, S.P., Kellogg, D.R., Tallada, V.A., Daga, R.R., and Jimenez, J. (2015). Nucleocytoplasmic transport in the midzone membrane domain controls yeast mitotic spindle disassembly. J. Cell Biol. 209, 387–402. https://doi.org/10.1083/jcb.201412144.

19. Yamamoto, A., Kitamura, K., Hihara, D., Hirose, Y., Katsuyama, S., and Hiraoka, Y. (2008). Spindle checkpoint activation at meiosis I advances anaphase II onset via meiosis-specific APC/C regulation. J. Cell Biol. 182, 277–288. https://doi.org/10.1083/jcb.200802053.

20. Hsu, K.S., and Toda, T. (2011). Ndc80 internal loop interacts with Dis1/TOG to ensure proper kinetochore-spindle attachment in fission yeast. Curr. Biol. 21, 214–220. https://doi.org/10.1016/j.cub.2010.12.048.

21. Yamashita, A., Sakuno, T., Watanabe, Y., and Yamamoto, M. (2017). Live Imaging of Chromosome Segregation during Meiosis in the Fission Yeast Schizosaccharomyces pombe. Cold Spring Harb. Protoc. 2017. pdb.prot091769. https://doi.org/10.1101/pdb.prot091769.

22. Saitoh, S., Takahashi, K., and Yanagida, M. (1997). Mis6, a fission yeast inner centromere protein, acts during G1/S and forms specialized chromatin required for equal segregation. Cell 90, 131–143. https://doi.org/10.1016/s0092-8674(00)80320-7.

23. Cairo, G., MacKenzie, A.M., and Lacefield, S. (2020). Differential requirement for Bub1 and Bub3 in regulation of meiotic versus mitotic chromosome segregation. J. Cell Biol. 219, e201909136. https://doi.org/10.1083/jcb.201909136.

24. Walczak, C.E., Cai, S., and Khodjakov, A. (2010). Mechanisms of chromosome behaviour during mitosis. Nat. Rev. Mol. Cell Biol. 11, 91–102. https://doi.org/10.1038/nrm2832.

25. Musacchio, A., and Salmon, E.D. (2007). The spindle-assembly checkpoint in space and time. Nat. Rev. Mol. Cell Biol. 8, 379–393. https://doi.org/10.1038/nrm2163.

26. Lara-Gonzalez, P., Pines, J., and Desai, A. (2021). Spindle assembly checkpoint activation and silencing at kinetochores. Semin. Cell Dev. Biol. 117, 86–98. https://doi.org/10.1016/j.semcdb.2021.06.009.

27. Marston, A.L., and Wassmann, K. (2017). Multiple Duties for Spindle Assembly Checkpoint Kinases in Meiosis. Front. Cell Dev. Biol. 5, 109. https://doi.org/10.3389/fcell.2017.00109.

28. Raina, V.B., Schoot Uiterkamp, M., and Vader, G. (2023). Checkpoint control in meiotic prophase: Idiosyncratic demands require unique characteristics. Curr. Top. Dev. Biol. 151, 281–315. https://doi.org/10.1016/bs.ctdb.2022.04.007.

29. Sakuno, T., Tanaka, K., Hauf, S., and Watanabe, Y. (2011). Repositioning of aurora B promoted by chiasmata ensures sister chromatid mono-orientation in meiosis I. Dev. Cell 21, 534–545. https://doi.org/10.1016/j.devcel.2011.08.012.

30. Watanabe, Y., and Nurse, P. (1999). Cohesin Rec8 is required for reductional chromosome segregation at meiosis. Nature 400, 461–464. https://doi.org/10.1038/22774.

31. Heinrich, S., Windecker, H., Hustedt, N., and Hauf, S. (2012). Mph1 kinetochore localization is crucial and upstream in the hierarchy of spindle assembly checkpoint protein recruitment to kinetochores. J. Cell Sci. 125, 4720–4727. https://doi.org/10.1242/jcs.110387.

32. Peters, J.M. (2006). The anaphase promoting complex/cyclosome: a machine designed to

destroy. Nat. Rev. Mol. Cell Biol. *7*, 644–656. https://doi.org/10.1038/nrm1988.

33. Lampson, M.A., and Cheeseman, I.M. (2011). Sensing centromere tension: Aurora B and the regulation of kinetochore function. Trends Cell Biol. *21*, 133–140. https://doi.org/10.1016/j.tcb.2010.10.007.

34. Santaguida, S., Vernieri, C., Villa, F., Ciliberto, A., and Musacchio, A. (2011). Evidence that Aurora B is implicated in spindle checkpoint signalling independently of error correction. EMBO J. *30*, 1508–1519. https://doi.org/10.1038/emboj.2011.70.

35. Vader, G., Cruijsen, C.W.A., van Harn, T., Vromans, M.J.M., Medema, R.H., and Lens, S.M.A. (2007). The chromosomal passenger complex controls spindle checkpoint function independent from its role in correcting microtubule kinetochore interactions. Mol. Biol. Cell *18*, 4553–4564. https://doi.org/10.1091/mbc.e07-04-0328.

36. Hauf, S., Biswas, A., Langegger, M., Kawashima, S.A., Tsukahara, T., and Watanabe, Y. (2007). Aurora controls sister kinetochore mono-orientation and homolog bi-orientation in meiosis-I. EMBO J. *26*, 4475–4486. https://doi.org/10.1038/sj.emboj.7601880.

37. Meyer, R.E., Kim, S., Obeso, D., Straight, P.D., Winey, M., and Dawson, D.S. (2013). Mps1 and Ipl1/Aurora B act sequentially to correctly orient chromosomes on the meiotic spindle of budding yeast. Science *339*, 1071–1074. https://doi.org/10.1126/science.1232518.

38. Yu, H.G., and Koshland, D. (2007). The Aurora kinase Ipl1 maintains the centromeric localization of PP2A to protect cohesin during meiosis. J. Cell Biol. *176*, 911–918. https://doi.org/10.1083/jcb.200609153.

39. Carmena, M., Wheelock, M., Funabiki, H., and Earnshaw, W.C. (2012). The chromosomal passenger complex (CPC): from easy rider to the godfather of mitosis. Nat. Rev. Mol. Cell Biol. *13*, 789–803. https://doi.org/10.1038/nrm3474.

40. Petersen, J., Paris, J., Willer, M., Philippe, M., and Hagan, I.M. (2001). The S. pombe aurora-related kinase Ark1 associates with mitotic structures in a stage dependent manner and is required for chromosome segregation. J. Cell Sci. *114*, 4371–4384. https://doi.org/10.1242/jcs.114.24.4371.

41. Leverson, J.D., Huang, H.K., Forsburg, S.L., and Hunter, T. (2002). The Schizosaccharomyces pombe aurora-related kinase Ark1 interacts with the inner centromere protein Pic1 and mediates chromosome segregation and cytokinesis. Mol. Biol. Cell *13*, 1132–1143. https://doi.org/10.1091/mbc.01-07-0330.

42. van der Horst, A., and Lens, S.M.A. (2014). Cell division: control of the chromosomal passenger complex in time and space. Chromosoma *123*, 25–42. https://doi.org/10.1007/s00412-013-0437-6.

43. Broad, A.J., and DeLuca, J.G. (2020). The right place at the right time: Aurora B kinase localization to centromeres and kinetochores. Essays Biochem. *64*, 299–311. https://doi.org/10.1042/ebc20190081.

44. Giet, R., and Glover, D.M. (2001). Drosophila aurora B kinase is required for histone H3 phosphorylation and condensin recruitment during chromosome condensation and to organize the central spindle during cytokinesis. J. Cell Biol. *152*, 669–682. https://doi.org/10.1083/jcb.152.4.669.

45. Terada, Y., Tatsuka, M., Suzuki, F., Yasuda, Y., Fujita, S., and Otsu, M. (1998). AIM-1: a mammalian midbody-associated protein required for cytokinesis. EMBO J. *17*, 667–676. https://doi.org/10.1093/emboj/17.3.667.

46. Tanaka, T.U. (2010). Kinetochore-microtubule interactions: steps towards bi-orientation. EMBO J. *29*, 4070–4082. https://doi.org/10.1038/emboj.2010.294.

47. Cesario, J.M., Jang, J.K., Redding, B., Shah, N., Rahman, T., and McKim, K.S. (2006). Kinesin 6 family member Subito participates in mitotic spindle assembly and interacts with mitotic regulators. J. Cell Sci. *119*, 4770–4780. https://doi.org/10.1242/jcs.03235.

48. Gruneberg, U., Neef, R., Honda, R., Nigg, E.A., and Barr, F.A. (2004). Relocation of Aurora B from centromeres to the central spindle at the metaphase to anaphase transition requires MKlp2. J. Cell Biol. *166*, 167–172. https://doi.org/10.1083/jcb.200403084.

49. Krüger, L.K., Gélin, M., Ji, L., Kikuti, C., Houdusse, A., Théry, M., Blanchoin, L., and Tran, P.T. (2021). Kinesin-6 Klp9 orchestrates spindle elongation by regulating microtubule sliding and growth. Elife *10*, e67489. https://doi.org/10.7554/eLife.67489.

50. Meadows, J.C., Lancaster, T.C., Buttrick, G.J., Sochaj, A.M., Messin, L.J., Del Mar Mora-Santos, M., Hardwick, K.G., and Millar, J.B.A. (2017). Identification of a Sgo2-Dependent but Mad2-Independent Pathway Controlling Anaphase Onset in Fission Yeast. Cell Rep. *18*, 1422–1433. https://doi.org/10.1016/j.celrep.2017.01.032.

51. Janson, M.E., Loughlin, R., Loïodice, I., Fu, C., Brunner, D., Nédélec, F.J., and Tran, P.T. (2007). Crosslinkers and motors organize dynamic microtubules to form stable bipolar arrays in fission yeast. Cell *128*, 357–368. https://doi.org/10.1016/j.cell.2006.12.030.

52. Yamashita, A., Sato, M., Fujita, A., Yamamoto, M., and Toda, T. (2005). The roles of fission yeast ase1 in mitotic cell division, meiotic nuclear oscillation, and cytokinesis checkpoint signaling. Mol. Biol. Cell *16*, 1378–1395. https://doi.org/10.1091/mbc.e04-10-0859.

53. Zheng, F., Dong, F., Yu, S., Li, T., Jian, Y., Nie, L., and Fu, C. (2020). Klp2 and Ase1 synergize to maintain meiotic spindle stability during metaphase I. J. Biol. Chem. *295*, 13287–13298. https://doi.org/10.1074/jbc.RA120.012905.

54. Zimmerman, S., and Chang, F. (2005). Effects of {gamma}-tubulin complex proteins on microtubule nucleation and catastrophe in fission yeast. Mol. Biol. Cell *16*, 2719–2733. https://doi.org/10.1091/mbc.e04-08-0676.

55. Polakova, S., Benko, Z., Zhang, L., and Gregan, J. (2014). Mal3, the Schizosaccharomyces pombe homolog of EB1, is required for karyogamy and for promoting oscillatory nuclear movement during meiosis. Cell Cycle *13*, 72–77. https://doi.org/10.4161/cc.26815.

56. Bishop, A.C., Ubersax, J.A., Petsch, D.T., Matheos, D.P., Gray, N.S., Blethrow, J., Shimizu, E., Tsien, J.Z., Schultz, P.G., Rose, M.D., et al. (2000). A chemical switch for inhibitor-sensitive alleles of any protein kinase. Nature *407*, 395–401. https://doi.org/10.1038/35030148.

57. Berthezene, J., Reyes, C., Li, T., Coulon, S., Bernard, P., Gachet, Y., and Tournier, S. (2020). Aurora B and condensin are dispensable for chromosome arm and telomere separation during meiosis II. Mol. Biol. Cell *31*, 889–905. https://doi.org/10.1091/mbc.E20-01-0021.

58. Cimini, D. (2008). Merotelic kinetochore orientation, aneuploidy, and cancer. Biochim. Biophys. Acta *1786*, 32–40. https://doi.org/10.1016/j.bbcan.2008.05.003.

59. Tsuchiya, D., Gonzalez, C., and Lacefield, S. (2011). The spindle checkpoint protein Mad2 regulates APC/C activity during prometaphase and metaphase of meiosis I in Saccharomyces cerevisiae. Mol. Biol. Cell *22*, 2848–2861. https://doi.org/10.1091/mbc.E11-04-0378.

60. Iwabuchi, M., Ohsumi, K., Yamamoto, T.M., Sawada, W., and Kishimoto, T. (2000). Residual Cdc2 activity remaining at meiosis I exit is essential for meiotic M-M transition in Xenopus oocyte extracts. EMBO J. *19*, 4513–4523. https://doi.org/10.1093/emboj/19.17.4513.

61. Kitajima, T.S., Kawashima, S.A., and Watanabe, Y. (2004). The conserved kinetochore protein shugoshin protects centromeric cohesion during meiosis. Nature *427*, 510–517. https://doi.org/10.1038/nature02312.

62. Miyazaki, S., Kim, J., Sakuno, T., and Watanabe, Y. (2017). Hierarchical Regulation of Centromeric Cohesion Protection by Meikin and Shugoshin during Meiosis I. Cold Spring Harbor Symp. Quant. Biol. *82*, 259–266. https://doi.org/10.1101/sqb.2017.82.033811.

63. Vallot, A., Leontiou, I., Cladière, D., El Yakoubi, W., Bolte, S., Buffin, E., and Wassmann, K. (2018). Tension-Induced Error Correction and Not Kinetochore Attachment Status Activates the SAC in an Aurora-B/C-Dependent Manner in Oocytes. Curr. Biol. *28*, 130–139.e3. https://doi.org/10.1016/j.cub.2017.11.049.

64. Hassold, T., and Hunt, P. (2001). To err (meiotically) is human: the genesis of human aneuploidy. Nat. Rev. Genet. *2*, 280–291. https://doi.org/10.1038/35066065.

65. Schneider, C.A., Rasband, W.S., and Eliceiri, K.W. (2012). NIH Image to ImageJ: 25 years of image analysis. Nat. Methods *9*, 671–675. https://doi.org/10.1038/nmeth.2089.

66. Moreno, S., Klar, A., and Nurse, P. (1991). Molecular genetic analysis of fission yeast Schizosaccharomyces pombe. Methods Enzymol. *194*, 795–823. https://doi.org/10.1016/0076-6879(91)94059-l.

67. Bähler, J., Wu, J.Q., Longtine, M.S., Shah, N.G., McKenzie, A., 3rd, Steever, A.B., Wach, A., Philippsen, P., and Pringle, J.R. (1998). Heterologous modules for efficient and versatile PCR-based gene targeting in Schizosaccharomyces pombe. Yeast *14*, 943–951. https://doi.org/10.1002/(sici)1097-0061(199807)14:10<943::aid-yea292>3.0.co;2-y.

68. Bohnert, K.A., Chen, J.S., Clifford, D.M., Vander Kooi, C.W., and Gould, K.L. (2009). A link between aurora kinase and Clp1/Cdc14 regulation uncovered by the identification of a fission yeast borealin-like protein. Mol. Biol. Cell *20*, 3646–3659. https://doi.org/10.1091/mbc.e09-04-0289.

STAR★METHODS

KEY RESOURCES TABLE

REAGENT or RESOURCE	SOURCE	IDENTIFIER
Chemicals, peptides, and recombinant proteins		
1-NM-PP1	Santa Cruz Biotechnology	SC-203214
Glycine max lectin	Sigma	L1395
Experimental models: Organisms/strains		
A list of *S. pombe* strains used in this study can be found in Table S1.	N/A	N/A
Oligonucleotides		
A list of the oligonucleotides used in this study can be found in Table S2.	N/A	N/A
Recombinant DNA		
pFA6a-GFP(S65T)-kanMX6	J. Bähler	pFA6a-GFP(S65T)-kanMX6
pFA6a- kanMX6	J. Bähler	pFA6a- kanMX6
pFA6a-mTurq2-natMX6	M. Sato	pFA6a-mTurq2-natMX6
Software and algorithms		
ImageJ	Schneider et al. 2012[65]	https://imagej.net/software/fiji/
Graphpad Prism 8.0.	Graphpad Software	https://www.graphpad.com
BioRender	BioRender Software	https://www.biorender.com
Other		
μ-Slide 8 well	Ibidi	Cat#: 80826
FCS2 chamber	Bioptechs	Cat#: 060319-2-03

RESOURCE AVAILABILITY

Lead contact

Further information and requests for resources, strains and reagents should be directed to and will be fulfilled by the lead contact, Juan Jimenez (jimmar@upo.es).

Materials availability

Plasmids and strains generated are available upon request to the lead contact.

Data and code availability

- All data reported in this paper will be shared by the lead contact upon request.
- This paper does not report original code.
- Any additional information required to reanalyze the data reported in this work paper is available from the lead contact upon request.

EXPERIMENTAL MODEL AND STUDY PARTICIPANT DETAILS

S. pombe strains and culture

Genotypes of strains used or built in this study can be found in Table S1. The growth and genetics of *S. pombe* were conducted using established methods.[66] In homothallic *S. pombe* h^{90} strains, isogenic daughter cells from germinating spores switch their mating type undergoing frequent conjugation-sporulating cycles at sporulation conditions. Taking advantage of this characteristic, h^{90} strains were used to examine spindle dynamics and chromosome segregation during meiotic divisions in zygotes with different mutant backgrounds. Deletions and strains expressing proteins tagged with GFP, mCherry, mTomato, or mTurquoise2 were generated and confirmed by PCR, following previous protocols.[67] Ark1-GFP tagging was checked by comparing the fluorescent signal with that of the KGY7900 strain (Ark1-GFP h+) from the K. Gould lab.[68] Double or multiple mutants were produced through mating, tetrad dissection, and selection based on drug resistance, auxotrophy markers, or the presence of fluorescent markers under the microscope. In general, yeast cells were grown in YES media. When selecting an auxotrophic mutant, minimal media without the supplement was used. Generally, the growth temperature for *S. pombe* was 30°C. Live-cell imaging was performed on h^{90} strains that were grown in YES media at 25°C for 18–24 hours. Meiosis was induced by transferring

cells to sporulation plates (SPA) and incubating them at 28°C for 10-12 hours until enough cells had mated. For all imaging assays, cells were cultured in SPA liquid media with supplements. Aurora B kinase inhibition assays were performed by adding 10 µM of the ATP analog 1-NM-PP1 to the imaging media.

METHOD DETAILS

Aurora B kinase inhibition assays

To evaluate Aurora B kinase inhibition, we utilized the *ark1-as3* analog-sensitive allele,[36] which enables specific and rapid deactivation of Aurora kinase via the ATP analog 1-NM-PP1. To selectively inhibit Aurora during meiosis II, we mounted cells in a µ-Slide eight-well chamber (Ibidi, 80826) previously coated with 100 µL of 1 mg/mL soybean lectin (Sigma-Aldrich, L1395) and added 10 µM of 1-NM-PP1 (Santa Cruz Biotechnology, SC-203214) to the imaging media after 10 minutes of time-lapse imaging. We focused our observations on cells that had initiated meiosis II (n between 170 and 376) to ensure that we captured only those cells that had undergone accurate chromosome segregation in meiosis I. To ensure that we had enough MII divisions, we selected those fields through the visualization of microtubules (mCherry-Atb2) where there was at least one cell at metaphase I-anaphase I. This ensured that when adding the inhibitor, this cell was on the verge of beginning meiosis II.

Live-cell microscopy

For live-cell imaging, cells were mounted in a Bioptechs FCS2 chamber using SPA liquid media (1% glucose, 7.3 mM KH2PO4, vitamins and 45 mg/L adenine, histidine, leucine, lysine, and uracil). To compare fluorescent signals between two or more strains, they were stuck in next, but separate drops of lectin so that the capturing settings and possible bleaching are identical between the control and experimental strains. The images were obtained using a spinning-disk confocal microscope (IX-81, Olympus; CoolSNAP HQ2 camera, Plan Apo-chromat 100x, 1.4 NA objective, Roper Scientific) and Metamorph software, with the temperature maintained at 25°C. Time-lapse images were captured at intervals of 2 or 5 minutes, with 20 slices with a Z step of 0.35 µm, every time point over a period of 5-6 hours.

For 3-color fluorescence analysis (refer to Figures 2D, 3A, and S4), images were acquired using a Zeiss Observer 7 inverted microscope equipped with Zeiss Plan-Apochromat 63X/1.40 Oil DIC and Alpha Plan-Apochromat 100x/1.46 Oil DIC lenses, coupled with a spinning Disk Confocal Yokogawa CSU-W1 head with excitation lasers and filters from 3i (Intelligent Imaging Innovations). Device control and image capture were performed using SlideBook6 software.

Image analysis and measurement of spindle and chromosome dynamics

The analysis of image stacks was conducted using ImageJ software. Maximum intensity projections were generated for subsequent analysis. To evaluate chromosome segregation at meiosis II, only cells with accurate chromosome segregation during meiosis I were selected for analysis. The duration of prometaphase and metaphase was determined by measuring spindle polymerization dynamics (mCherry-Atb2). Specifically, we measured the duration of phase I, during which the spindle elongates as a short spindle, and phase II, during which the spindle remains relatively constant in length. Anaphase onset was identified as the beginning of phase III, during which the spindle further elongates and eventually disappears.

QUANTIFICATION AND STATISTICAL ANALYSIS

Quantification of fluorescent signals

The fluorescence intensity was measured by defining a region of interest around the targeted area and subtracting fluorescence within an equivalent background area. To analyze fluorescence intensity dynamics, a region of interest was traced and the average intensity per pixel was calculated while subtracting the background over time. To maintain consistency, the fluorescence images of both the wild-type and mutant samples were acquired simultaneously.

Statistical analysis

Graphs and statistical analyses were generated using Microsoft Excel and Prism 8.0 (GraphPad Software). The mean and standard deviation (SD) are represented in the graphs, and the number of cells scored from at least three independent experiments is indicated as n. Two-group comparisons were performed using unpaired Student's t-test, while multiple-group comparisons were analyzed using non-parametric Kruskal-Wallis one-way ANOVA and ordinary one-way ANOVA. Chi-square tests were utilized to compare the frequencies of phenotypes between conditions in Figures 4C, 5B, and 5C. Statistical significance was considered for p-values lower than 0.05 (*). Further details of statistical analysis are given in the figure legends.